Effects of Structural Nonlinearities on Flutter Characteristics of the CF-18 Aircraft

B. H. K. Lee* and A. Tron†
National Research Council, Ottawa, Ontario, Canada

The describing function method is used to analyze the flutter characteristics of the CF-18 aircraft with structural nonlinearities. The first nonlinearity studied is located at the CF-18 wing-fold hinge. From ground test data, this hinge can be represented by a bilinear spring. A flutter sensitivity study is carried out, which shows that when the hinge stiffness is reduced, divergent flutter involving the wing bending and torsion modes is replaced by limit-cycle flutter of the wing torsion and outer wing rotation modes. Another form of nonlinearity at the outboard leading-edge flap is also studied by treating it as a spring with free-play. Limit-cycle oscillations are possible only within a small range of velocities in the vicinity of its linear flutter velocity. The flutter modes remain unchanged and their frequencies are practically constant for hinge-stiffness values ranging from a few percent to its nominal value. Positive aileron angles are found to be more effective in alleviating limit-cycle flutter at the wing-fold than negative angles. Similar observations are made at the outboard leading-edge flap hinge where downward deflection of the aileron gives larger values of the preload and, hence, the equivalent stiffness than upward deflection.

Nomenclature

A = maximum positive displacement from equilibrium position
A_0 = midpoint of oscillation of nonlinear spring
A_1 = amplitude of oscillation measured from A_0
K_e = equivalent spring stiffness
K_1, K_2 = stiffnesses of bilinear spring
M = load
M_1 = amplitude of sinusoidal load
P = preload
$2S$ = region where softer spring acts
AIL = aileron
LEF = leading-edge flap
TEF = trailing-edge flap
t = time
x = displacement
x_1 = amplitude of sinusoidal displacement
ω = frequency

Introduction

THE assumption of structural linearity is frequently made to determine the divergence and flutter characteristics of aerodynamic surfaces. Linear theory predicts the magnitude of dynamic pressure or flight velocity above which the system under consideration becomes unstable and the motion grows exponentially in time. However, aircraft structures often exhibit nonlinearities that affect not only the flutter speed but also the characteristics of flutter motion. References 1 and 2 give an excellent discussion of the various types of nonlinearities and some of the methods used to treat them. In general, they can be categorized as either distributed or concentrated. Only the latter is considered in this study, and the types investigated are the bilinear and free-play springs that represent worn or loose hinges of control surfaces. The hinge-stiffness behavior and the response characteristics are usually functions of the amplitude of oscillations so that at some particular flight speed the oscillations can be self-excited and can attain a limited amplitude. The appearance of the phenomenon of limit-cycle flutter is important from the design viewpoint. These oscillations may occur within the divergence and flutter flight envelope, and the amplitude, frequency and duration of these limit-cycle oscillations may have an important impact on the structural integrity of the aerodynamic surfaces.

Air-to-air photography and video coverage of recent flight tests of the CF-18 aircraft at the Aerospace Engineering Test Establishment at Canadian Forces Base (CFB) Cold Lake showed that the wing responses were severely affected by a decrease in the wing-fold hinge stiffness. With light-to-intermediate weight outboard stores and with tip missiles off, the aircraft was subjected to lightly damped low-frequency oscillations. In this paper, the effect of nonlinear wing-fold stiffness on limit-cycle oscillations is examined. Another nonlinearity at the outboard leading-edge-flap hinge, which may be important, is also investigated. A schematic of the locations of these two hinges on the CF-18 wing is given in Fig. 1. Nonlinearities in the trailing-edge flaps and ailerons are not considered because ground tests show they have little or no free-play.

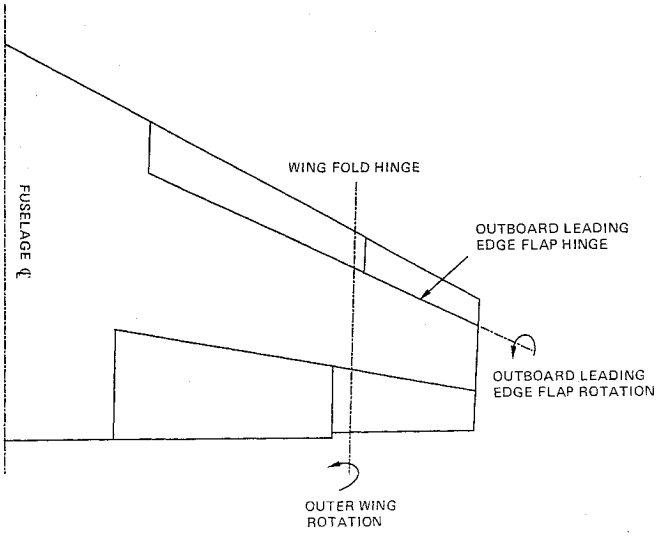

Fig. 1 Schematic of locations of wing-fold and outboard leading-edge flap hinges on the CF-18 wing.

Received Sept. 13, 1988; revision received Jan. 22, 1989.

*Senior Research Officer, High Speed Aerodynamics Laboratory, National Aeronautical Establishment. Member AIAA.

†High Speed Aerodynamics Laboratory, National Aeronautical Establishment; currently, Undergraduate Student, University of Waterloo.

The wing planform is extended to the fuselage centerline and the LEX (leading-edge extension) is not shown. The describing function approach in nonlinear mechanics is used to find the equivalent hinge stiffness and flutter analysis is then carried out with modal data computed using the equivalent stiffness.

The wing-fold and leading-edge hinges are represented in the NASTRAN[3] model of the CF-18 by discrete elements and modifications to the spring stiffness are rather straightforward. To change the preloads on the nonlinear springs, flaps can be employed to alter the aerodynamic moments acting on these hinges and, hence, move the equilibrium point anywhere along the moment vs deflection curves of the hinges. Combinations of the leading-edge flaps, trailing-edge flaps, and aileron angles are used and the hinge moments are calculated from a three-dimensional transonic wing/body computer code developed by Kafyeke.[4] The computations are carried out for an aircraft configuration and flight conditions that correspond to one of the worst cases where limit-cycle oscillations were observed in flight tests.

Equivalent Stiffness Approximations

The describing function is a useful technique in treating structural nonlinearities by evaluating an equivalent stiffness. The dynamic system can then be linearized and the usual linear flutter-analysis methods can be applied. The basic approach for the method is to assume that the displacement is sinusoidal and of the form

$$x = x_1 \sin \omega t \tag{1}$$

Using this expression, the load developed in the nonlinear spring is expanded in a Fourier series. The higher harmonic terms are neglected and the load is expressed as

$$M = M_1 \sin \omega t \tag{2}$$

The ratio of M_1/x_1 gives the equivalent stiffness of the spring.

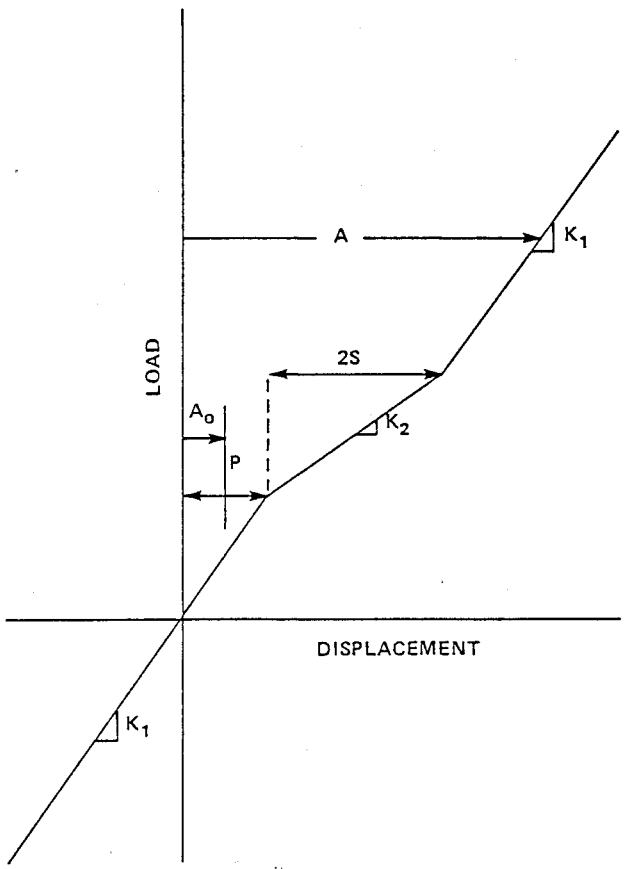

Fig. 2 Schematic of a bilinear spring with preload.

The types of nonlinearities being treated in this study are the bilinear spring and the free-play spring, which is a special case of the former when the stiffness of the softer spring K_2 (Fig. 2) is set equal to zero. Using the method given by Laurenson et al.,[5] the equivalent stiffness K_e of a bilinear spring with

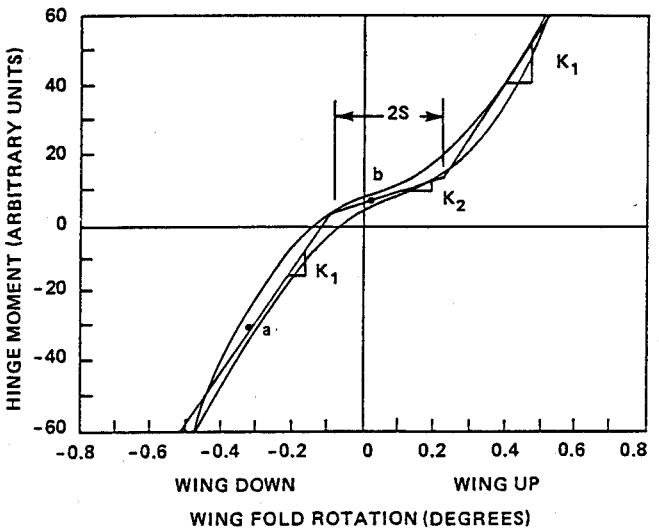

Fig. 3a Moment vs wing-fold hinge rotation at small deflection angles.

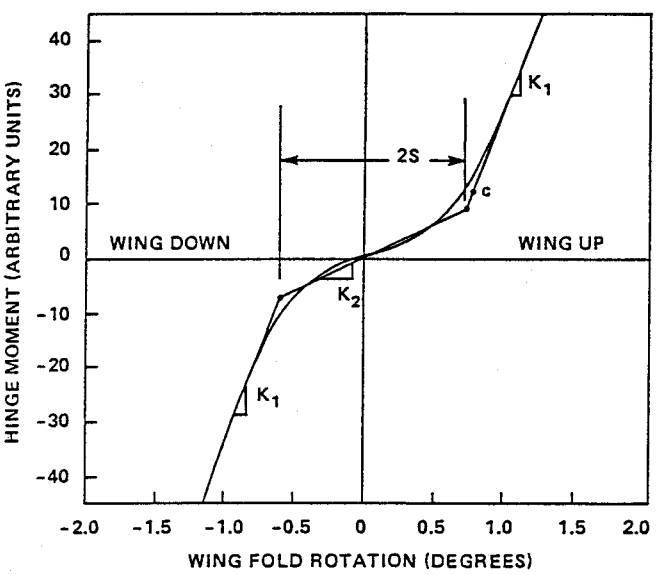

Fig. 3b Moment vs wing-fold hinge rotation at large deflection angles.

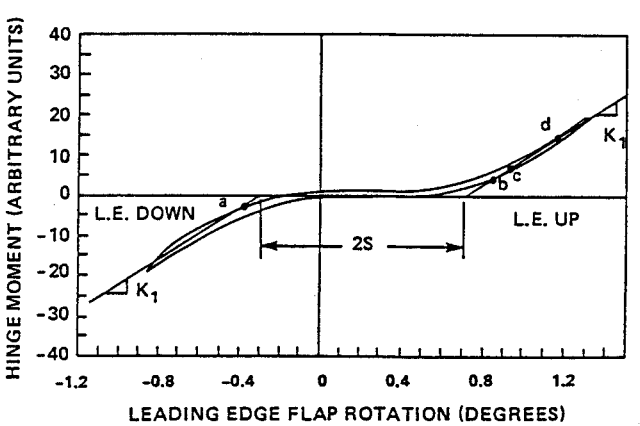

Fig. 3c Moment vs leading-edge flap rotation.

preload can be derived to first-order accuracy as

$$K_e = K_1, \quad \text{for } A \le P$$

$$= \frac{1}{\pi}\left\{K_1\pi + (K_2 - K_1)t_1 + 2(K_1 - K_2)\left(\frac{P - A_0}{A_1}\right)\sin t_1 + \left(\frac{K_2 - K_1}{2}\right)\sin 2t_1\right\}, \quad \text{for } P \le A \le P + 2S$$

$$= \frac{1}{\pi}\left\{2(K_1 - K_2)\left(\frac{P - A_0}{A_1}\right)\sin t_1 + (K_2 - K_1)t_1 + 2(K_2 - K_1)\left(\frac{P + 2S - A_0}{A_1}\right)\sin t_2 + (K_1 - K_2)t_2 + \frac{K_2 - K_1}{2}(\sin 2t_1 - \sin 2t_2) + K_1\pi\right\}, \quad \text{for } A \ge P + 2S \quad (3)$$

where

$$t_1 = \cos^{-1}\left(\frac{P - A_0}{A_1}\right)$$

$$t_2 = \cos^{-1}\left(\frac{P + 2S - A_0}{A_1}\right)$$

$$A = A_0 + A_1$$

$$A_0 = 0, \quad A \le P$$

$$= \frac{A}{2} - \frac{1}{2}\sqrt{A^2 - \frac{K_1 - K_2}{K_1}(P - A)^2}, \quad P \le A \le P + 2S$$

$$= \frac{A}{2} - \frac{1}{2}\sqrt{A^2 - 4S\left(\frac{K_1 - K_2}{K_1}\right)(A - P - S)}$$

$$A \ge P + 2S \quad (4)$$

From ground testing of the CF-18, a typical curve[6] of the hinge moment vs wing-fold rotation is given in Fig. 3a. A small amount of hysteresis is present, but it is neglected in this investigation and the nonlinearity is treated as a bilinear spring. For amplitudes of the wing-fold motion greater than 0.4 deg with reference to the ground-test equilibrium position, the spring is approximated as in Fig. 3b, where K_1 has a magnitude equal to its design value. The values of the range $2S$ and stiffnesses K_1 and K_2 are different in these two figures. Figure 3c shows a typical experimental moment-displacement curve[6] for the outboard leading-edge hinge. Again, the small amount of hysteresis is neglected and the nonlinearity is treated as a free-play. For sinusoidal displacements, the analysis given by Shen[2] for treating hysteresis can be used to determine the moment versus time curves. For small amount of hysteresis as shown in Figs. 3a and 3c, the curves are very similar to those for bilinear or free-play springs. Hence, neglecting hysteresis in the hinges considered in this study should not introduce any significant errors in the results.

Figures 3a–3c are obtained from ground tests and can be used to determine the equivalent stiffness at given flight conditions. Before Eq. (3) can be used, the aerodynamic loading on these hinges must be determined in order to locate the equilibrium position, and, hence, the value of the preload. Using a test point corresponding to a 1-g level flight at Mach number of 0.95 and an altitude of 7000 ft above sea level, the steady transonic wing/body computer code of Ref. 4 is used to compute hinge moments for various combinations of the flaps and aileron settings. In order to maintain a fixed lift coefficient for the aircraft, the angle of attack has to be computed for each flaps-aileron combination. For the wing-fold hinge, flutter results for three cases will be presented later on, and they are denoted by a, b, and c in Fig. 3a and 3b. The flaps and aileron deflection angles are given in Table 1a. Four preload values are used to analyze the outboard leading-edge flap free-play spring and they are indicated by points a to d in Fig. 3c. The flaps-aileron settings corresponding to these four points are shown in Table 1b.

The equivalent stiffnesses of these two hinges for the flaps-aileron settings given above are shown in Fig. 4. In Fig. 4a, the range $2S$ and the stiffnesses K_1 and K_2 are similar for cases a and b, but they are different from case c. The normalizing factor is the same and it is the value of the linear design wing-fold hinge stiffness. For the outboard leading-edge flap hinge, the equivalent stiffness shown in Fig. 4b is nondimensionalized by its nominal value.

Nonlinear Hinge Stiffness Sensitivity Analysis

Wing-Fold Hinge

Only one CF-18 aircraft configuration, which has been shown to be subject to limit-cycle oscillations in flight tests, is analyzed. In carrying out a wing-fold hinge-stiffness sensitivity study, a wing-fold stiffness is specified and a NASTRAN[3] modal analysis is performed to give the generalized masses, stiffnesses, and vibrational modes. Using the first 23 modes,

Table 1 Flaps-aileron combinations for hinge moment calculations

Case	Trailing-edge flap angle, deg	Aileron angle, deg	Leading-edge flap angle, deg
a) Wing-fold hinge nonlinearity			
a	1	−4	2
b	1	−2	−3
c	1	4	0
b) Outboard leading-edge flap hinge nonlinearity			
a	1	−4	0
b	1	4	−3
c	1	2	−3
d	1	−2	−3

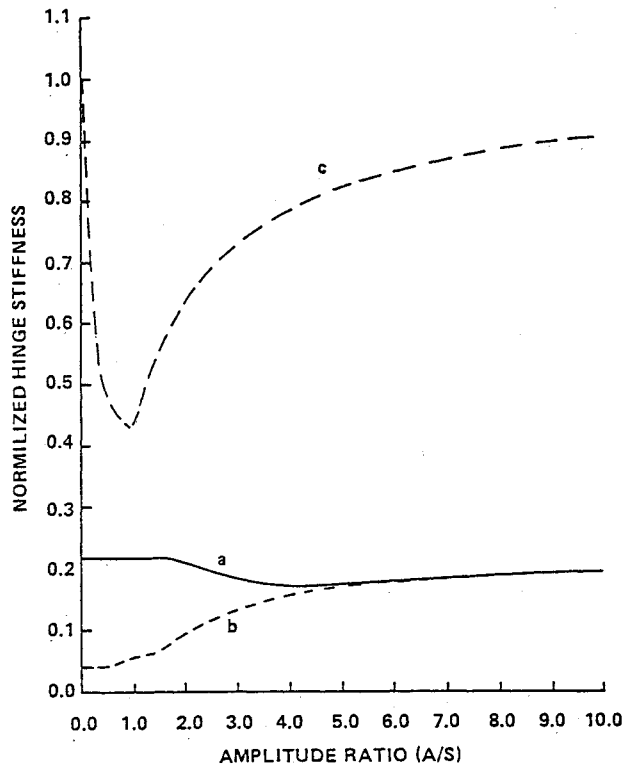

Fig. 4a Normalized equivalent wing-fold hinge stiffness vs amplitude ratio at flaps-aileron settings: a) AIL = −4 deg, LEF = 2 deg; b) AIL = −2 deg, LEF = −3 deg; c) AIL = 4 deg, LEF = 0 deg. TEF is fixed at 1 deg.

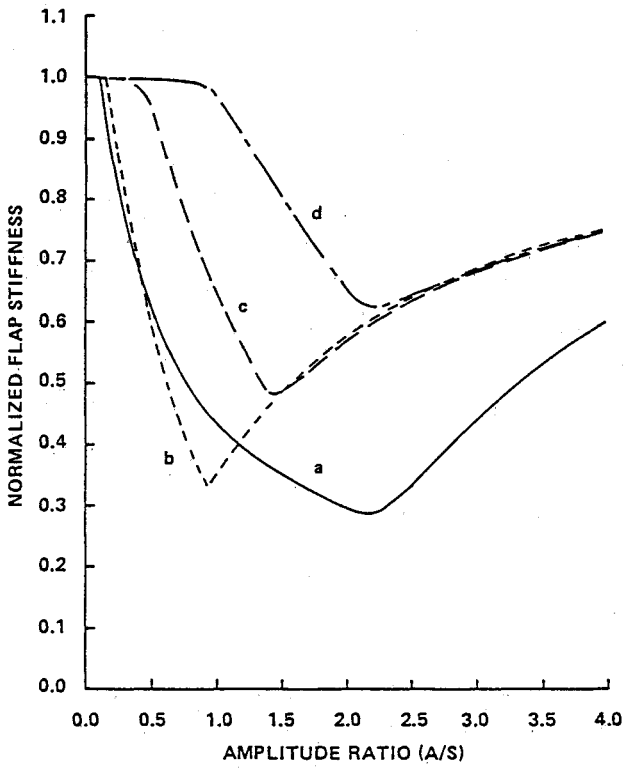

Fig. 4b Normalized equivalent outboard leading-edge flap hinge stiffness vs amplitude ratio at flaps-aileron settings: a) AIL = −4 deg, LEF = 0 deg; b) AIL = 4 deg, LEF = −3 deg; c) AIL = 2 deg, LEF = −3 deg; d) AIL = −2 deg, LEF = −3 deg. TEF is fixed at 1 deg.

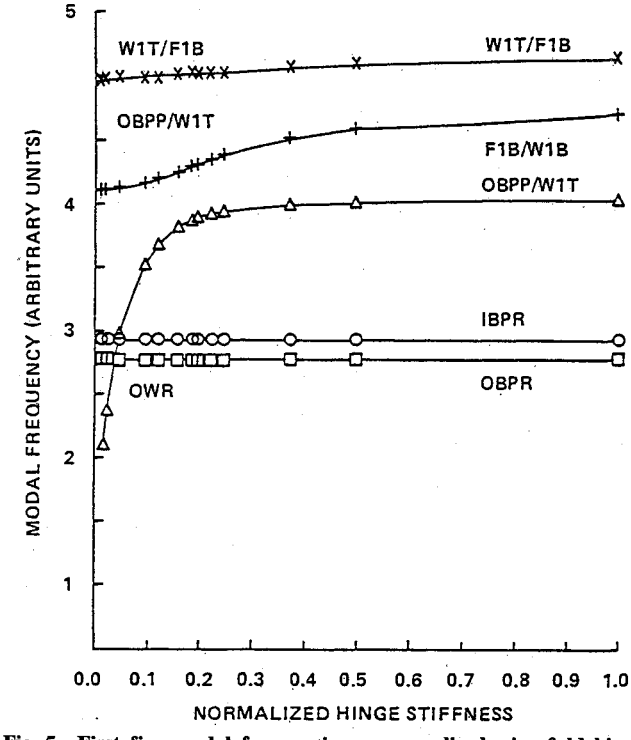

Fig. 5 First five modal frequencies vs normalized wing-fold hinge stiffness.

the generalized forces are computed from a doublet-lattice[7] aerodynamics computer program, which forms part of the flutter analysis code used at the National Aeronautical Establishment. The structural damping for these modes determined from ground-vibration tests are inputed into the flutter code and the *V-g* method is used to evaluate matched point (Mach number and altitude) damping and frequency trends.

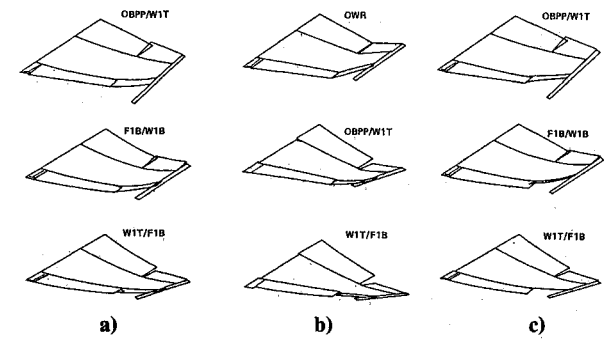

Fig. 6 Mode shapes for a) nominal stiffness values for both hinges; b) 10% of nominal wing-fold hinge stiffness value and nominal outer leading-edge flap hinge value; and c) nominal wing-fold hinge value and 2.8% of nominal leading-edge flap hinge stiffness.

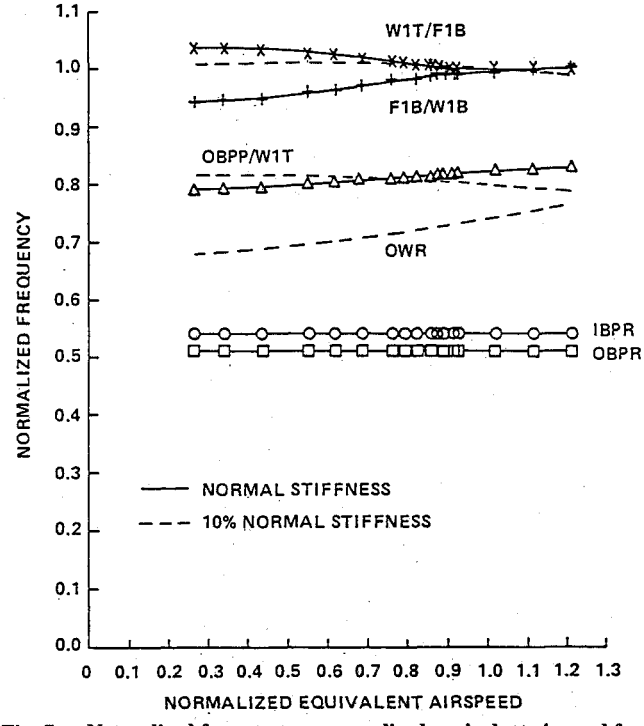

Fig. 7a Normalized frequency vs normalized equivalent airspeed for normalized wing-fold hinge stiffness values of 1 and 0.1.

Figure 5 shows the effect of reducing the wing-fold stiffness on the modal frequencies for the first five antisymmetric modes. The inboard and outboard store roll modes designated as IBSR and OBSR are relatively unaffected by changes in the hinge stiffness. As the stiffness is reduced, the outboard store pitch/wing first torsion (OBSP/W1T) mode is replaced by the outer wing rotation mode (OWR), and the wing first bending /fuselage first bending (W1B/F1B) mode changes to the OBSP/W1T mode. The mode shapes are shown in Fig. 6a using the nominal stiffness values for both hinges. Figure 6b shows that at 10% of the the nominal wing-fold stiffness value, the OBSP/W1T and W1B/F1B modes are replaced by the OWR and OBSP/W1T modes, respectively.

Figures 7a and 7b show the frequency and damping trends for normalized hinge stiffness values of 1 and 0.1, respectively. The airspeed and frequency are normalized by their respective flutter values calculated using the design value of the wing-fold stiffness. The flutter characteristics and the switching of the flutter modes are clearly indicated in these figures.

When the wing-fold hinge stiffness is decreased, the change in the frequency of the W1T/F1B mode is small. However, much larger decrease in the frequency of the W1B/F1B mode is detected. Because the frequency separation between these

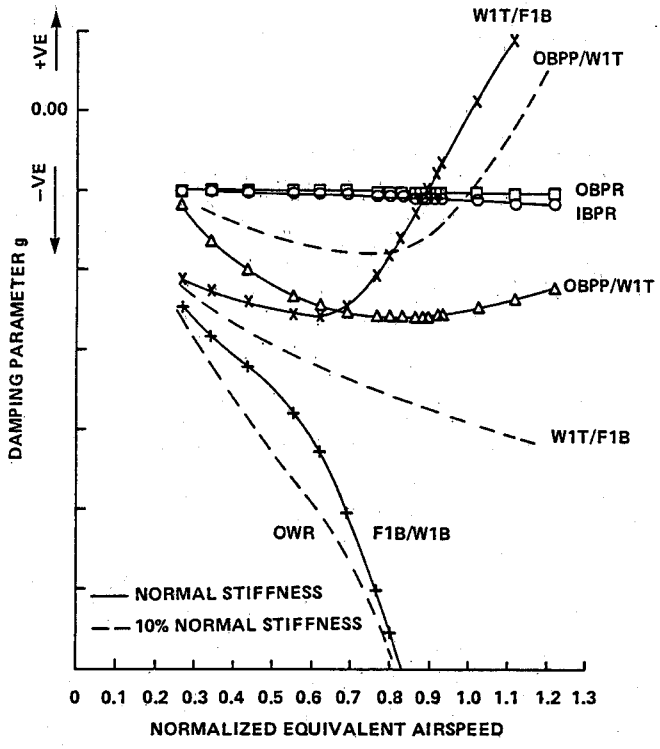

Fig. 7b Damping vs normalized equivalent airspeed for normalized wing-fold hinge stiffness values of 1 and 0.1.

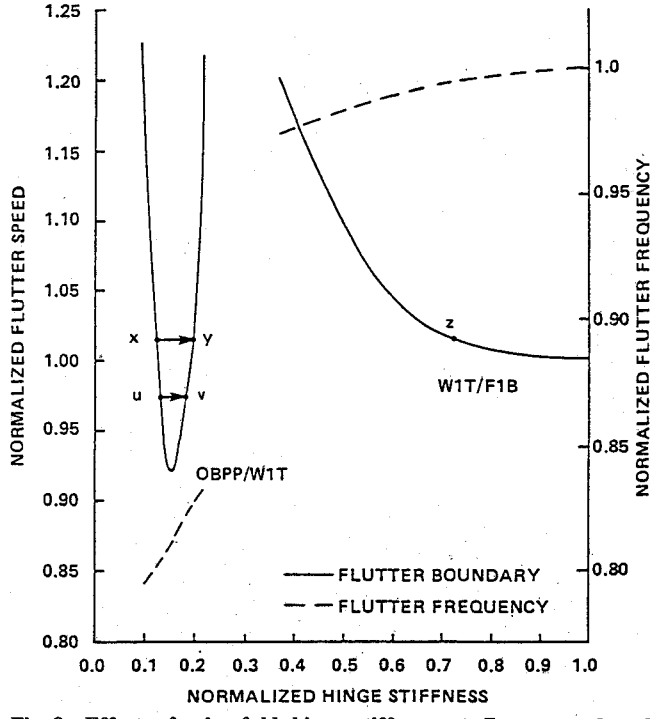

Fig. 8 Effect of wing-fold hinge stiffness on flutter speed and frequency.

two modes increases with decreasing wing-fold stiffness, flutter due to interaction of these two modes is found to occur at higher velocities. This is shown in Fig. 8 where higher flutter speeds and slightly lower frequencies of the flutter mode W1T/F1B are shown for decreasing value of the wing-fold stiffness. In the range of stiffness values where flutter changes to the OBSP/W1T mode, the flutter boundary has a minimum. Take as an example, point x in the figure. To the left, the motion is stable, but an increase in amplitude and, hence, spring stiffness will cause the motion to grow until point y is reached where the oscillations become limit-cycle. Any further

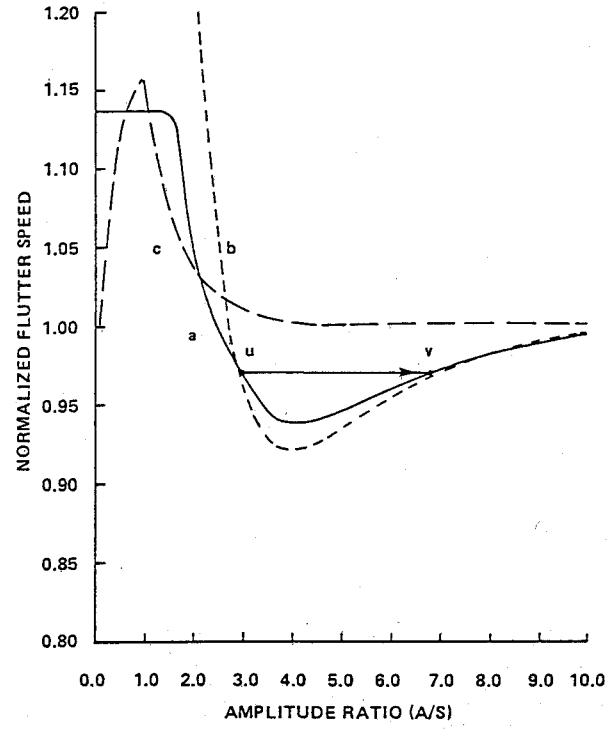

Fig. 9 Normalized flutter speed vs amplitude ratio for the wing-fold hinge at three flaps-aileron settings.

increase in amplitude or stiffness will be stable and the motion will return to point y. Beyond point z, the motion becomes divergent. Some similar observations for a two-degree-of-freedom flutter model are reported by Lee[8].

The normalized flutter speed is plotted in Fig. 9 against the amplitude ratio for three sets of flaps-aileron angles described earlier. For cases a and b, the equivalent stiffness shown in Fig. 3a is small and flutter is due to the interaction of the OBSP/W1T and OWR modes. A minimum velocity occurs at an amplitude ratio of approximately 4. The points u and v marked on the figure correspond to the same points in Fig. 8 that show limit-cycle flutter is possible. Increasing the steady-state hinge moment by changing the flaps-aileron angles to correspond to case c involves flutter between the W1T/F1B and W1B/F1B modes. An increase in flutter speed is observed with increasing amplitude since this corresponds to an initial decrease in spring stiffness. After the stiffness reaches a minimum (Fig. 4a), it increases with amplitude ratio with a resulting drop in flutter velocity. No limit-cycle oscillations are observed for this case and only divergent flutter can occur.

Outboard Leading-Edge Flap Hinge

From the NASTRAN analysis, it is found that the frequencies of the important modes are practically unchanged, even when the outboard leading-edge flap hinge stiffness is only a few percent of its nominal value. The three low-frequency modes that are important in flutter are plotted in Fig. 6c using a hinge stiffness of 2.8% of its nominal value. The mode shapes are quite similar to those in Fig. 6a with the exception of the outer leading-edge flap where large deflections are detected. This is to be expected since the hinge stiffness is very small.

Flutter always involves the W1T/F1B and W1B/F1B modes regardless of the value of hinge stiffness used. In Fig. 10, the normalized flutter speed and frequency are plotted against the normalized stiffness. Limit-cycle oscillations can occur in a small speed range between 0.975 and 1 for stiffnesses greater than 0.275. Oscillatory motion to the left of x will decay, while to the right of x, the amplitude will grow until it reaches y where limit-cycle flutter will occur. Any amplitude or hinge stiffness larger than that at y will decrease until it reaches the

value at y. Above a normalized flutter speed of 1.08, the region bounded by the curves r–s and t–u has a peculiar behavior since an initial motion with a given amplitude will decay until it reaches curve r–s, where any further decrease in amplitude or stiffness will result in divergent flutter. In the presence of steady-state aerodynamic loading, the equilibrium point of the outboard leading-edge flap hinge will fall outside the free play and the equivalent stiffness can be equal to or greater than 0.275. This value of the stiffness corresponds to point u in Fig. 10. Hence, for the four cases considered in this study which are shown in Fig. 3c, only the portion of the flutter boundary u–x–y–z is applicable.

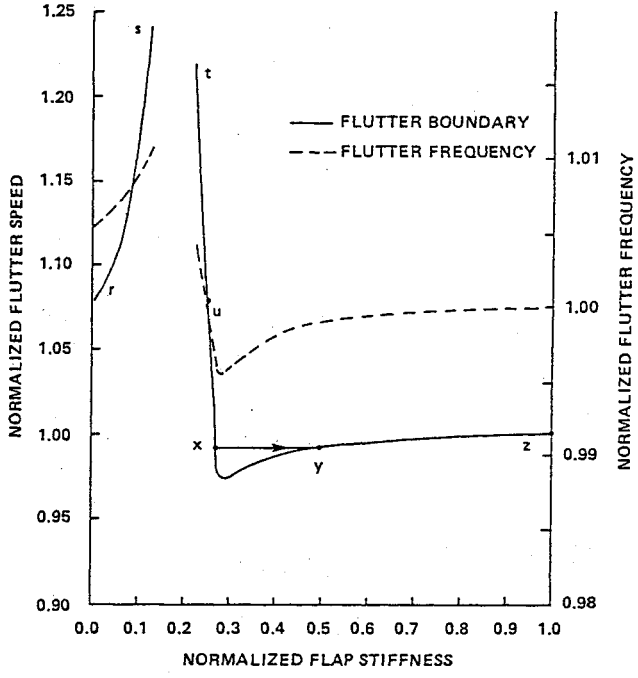

Fig. 10 Effect of outboard leading-edge flap hinge stiffness on flutter speed and frequency.

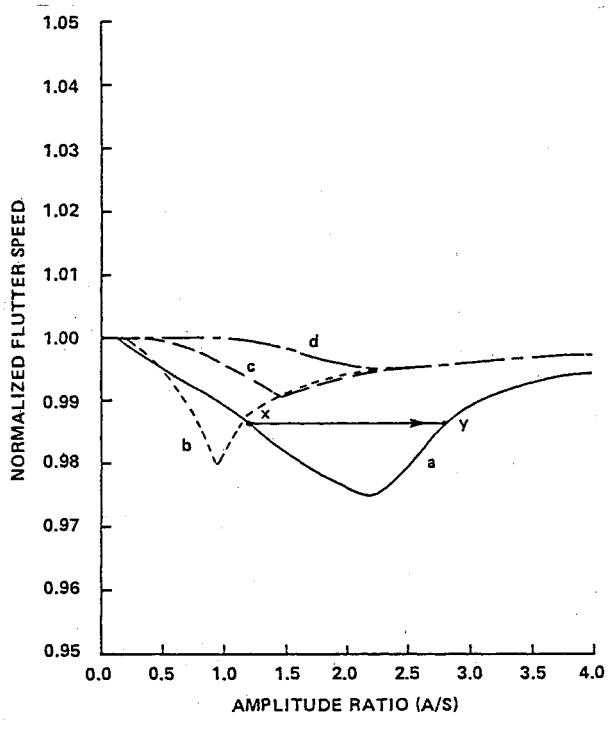

Fig. 11 Normalized flutter speed vs amplitude ratio for the leading-edge flap hinge at four flaps-aileron settings.

Figure 11 shows the normalized flutter speed vs amplitude ratio for the four flaps-aileron settings. As the hinge moment increases to larger values, the stiffness approaches its nominal value and the range of flutter speed, where limit-cycle oscillations can occur, diminishes until finally only divergent flutter is possible.

Conclusions

Analysis of the flutter characteristics of the CF-18 aircraft with structural nonlinearities can be dealt with quite effectively using the describing-function approach. With a nonlinearity of the type represented by a bilinear spring at the wing-fold hinge and with insufficient preload, binary flutter of the wing bending and torsion modes is replaced by the wing torsion and outer wing rotation modes. Limit-cycle oscillations can occur with considerable increase in flutter speed above that for nominal hinge stiffness.

Representing the outboard leading-edge flap hinge nonlinearity by a free play, it is shown that, using ground test data for the particular hinge under consideration, limit-cycle oscillations are possible within a small range of the normalized flutter speed from 0.975 to 1 for stiffnesses greater than 0.275 of its nominal value. The flutter modes remain unchanged even for very small values of the hinge stiffness, and modal analysis of the wing bending and torsion modes shows the frequencies to remain practically constant.

Positive aileron angles are more effective in alleviating limit-cycle flutter due to stiffness nonlinearity at the wing fold than negative angles. Similar observations are also made for the outboard leading-edge flap hinge, where downward deflection of the aileron gives larger values of the preload and, hence, stiffer values for the equivalent spring.

Acknowledgments

The authors wish to thank the Department of National Defence of Canada for their support under FE 220786NRC06 and for making available some CF-18 data.

References

[1]Brietbach, E., "Effect of Structural Nonlinearities on Aircraft Vibration and Flutter," AGARD Rept. 665, Jan. 1978.

[2]Shen, S. F., "An Approximate Analysis of Nonlinear Flutter Problems," *Journal of Aeronautical Sciences,* Vol. 26, Jan. 1959, pp. 25–32.

[3]*MSC/NASTRAN, User's Manual,* MacNeal-Schwendler Corp., Los Angeles, CA, 1981.

[4]Kafyeke, F., "An Analysis Method for Transonic Flow about Three-Dimensional Configurations," Canadair Ltd., Montreal, Canada, Rept. RAZ-000-516, Feb. 1986.

[5]Laurenson, R. M., Hauenstein, A. J., and Gubser, J. L., "Effects of Structural Nonlinearities on Limit-Cycle Response of Aerodynamic Surfaces," AIAA Paper 86-0899, May, 1986.

[6]Potter, M., Department of National Defence of Canada, Ottawa, Canada, Private Communication, 1985.

[7]Rodden, W. P., Giesing, J. P., and Kalman, T. P., "New Developments and Applications of the Subsonic Doublet-Lattice Method for Nonplanar Configurations," Paper No. 4, AGARD CP-80, Symposium on Unsteady Aerodynamics for Aeroelastic Analyses of Interfering Surfaces, May 1970.

[8]Lee, C. L., "An Iterative Procedure for Nonlinear Flutter Analysis," AIAA Paper 85-0688, April 1985.